Sliding charge-density wave in manganites

SUSAN COX[1]*, J. SINGLETON[1], R. D. McDONALD[1], A. MIGLIORI[1] AND P. B. LITTLEWOOD[2]

[1]National High Magnetic Field Laboratory, Ms-E536, Los Alamos National Laboratory, New Mexico 87545, USA

[2]Cavendish Laboratory, University of Cambridge, Cambridge, CB3 0HE, UK

*e-mail: scox@lanl.gov

Published online: 2 December 2007; doi:10.1038/nmat2071

Stripe and chequerboard phases appear in many metal oxide compounds, and are thought to be linked to exotic behaviour such as high-temperature superconductivity[1] and colossal magnetoresistance[2]. It is therefore extremely important to understand the fundamental nature of such phases. The so-called stripe phase of the manganites has long been interpreted as the localization of charge at atomic sites[3–6]. Here, we present resistance measurements on $La_{0.50}Ca_{0.50}MnO_3$ that strongly suggest that this state is in fact a prototypical charge-density wave (CDW) that undergoes collective transport. Dramatic resistance hysteresis effects and broadband noise properties are observed, both of which are typical of sliding CDW systems. Moreover, the high levels of disorder typical of manganites result in behaviour similar to that of well-known disordered CDW materials. The CDW-type behaviour of the manganite superstructure suggests that unusual transport and structural properties do not require exotic physics, but could emerge when a well-understood phase (the CDW) coexists with disorder.

The stripe phase in manganites of the form $La_{1-x}Ca_xMnO_3$ appears as the temperature is lowered through $T \simeq 240$ K, and the superstructure wavevector settles on a final value of $\mathbf{q} \simeq (1-x)\mathbf{a}^*$ (ref. 3) (where $\mathbf{a}^*$ is the reciprocal lattice vector) for $0.5 \leq x < 0.85$, at $T \simeq 120$ K (ref. 4). On the basis of the insulating nature of the manganites up to room temperature, and the observation of stripes of charge order in transmission electron microscopy (TEM) images, early studies concluded that the superstructure arose from localization of charge at atomic sites[5,6]. However, neutron and X-ray studies found the degree of charge localization at Mn sites to be small, and subsequent theoretical work suggested that a charge-density-wave (CDW) model may be more applicable[7]. This suggestion is supported by the observation that q/a^* is strongly temperature dependent[4,8], indicating that a model in which the superstructure periodicity is derived from the sample stoichiometry cannot be valid. In addition, heat capacity peaks at the transition to the stripe phase can be modelled as 'dirty Peierls transitions', as expected in a disordered CDW system[9]. However, the possibility of the stripe phase exhibiting sliding behaviour, as seen in many other CDW systems[10], could not be probed without the ability to make orientation-dependent resistivity measurements. Here, we describe the first such measurements on the manganite stripe phase, which reveal dramatic orientation-dependent resistivity and broadband noise effects that are characteristic of CDW sliding.

Orientation-dependent resistivity measurements require thin films, because untwinned single crystals of the insulating manganites cannot be grown[11]. The 80-nm-thick $La_{0.5}Ca_{0.5}MnO_3$ thin film was grown on a $NdGaO_3$ substrate as described in ref. 12. It should be noted that the $La_{0.5}Ca_{0.5}MnO_3$ thin-film phase diagram differs from the bulk polycrystalline phase diagram in that there is no intersection of the ferromagnetic and stripe phases at $x = 0.5$; instead, the ferromagnetic phase is present for $x < 0.42$; for $x > 0.42$, a paramagnetic insulating phase appears[13] (Fig. 1a, inset). The film was prepared for TEM by conventional grinding of the substrate to 50 μm and then milling a small window using a focused

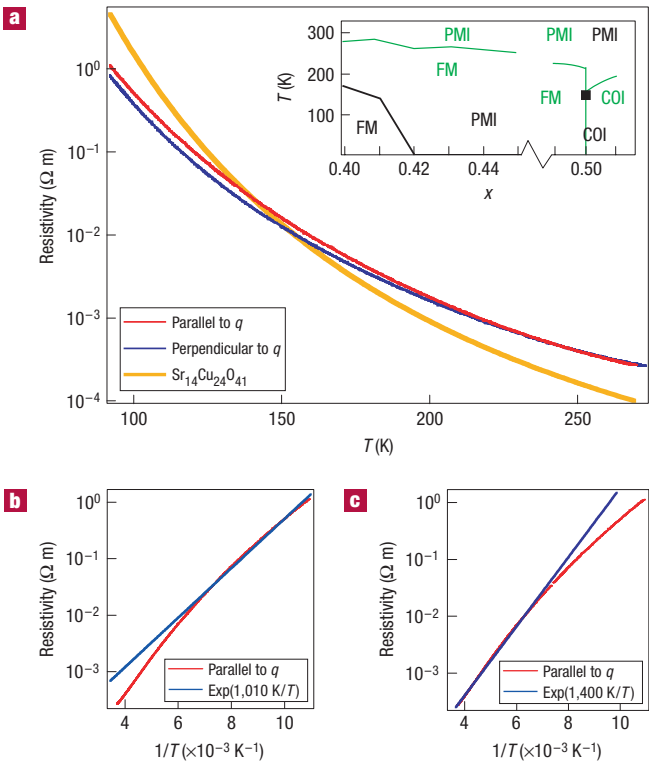

Figure 1 Variation of the differential resistance with temperature, demonstrating activated behaviour. a, Differential resistance of $La_{0.5}Ca_{0.5}MnO_3$ with the current in the **a** (red line) and **c** (blue line) directions versus temperature (zero d.c. bias). The resistivity is similar to that of the ladder compound $Sr_{14}Cu_{24}O_{41}$ (yellow line)[19]. Inset: Phase diagram of thin-film $La_{1-x}Ca_xMnO_3$ (in black), demonstrating that the ferromagnetic (FM) phase disappears at $x = 0.42$, and is replaced by the paramagnetic insulator (PMI) phase, whereas the charge-ordered insulating (COI) phase is present at $x = 0.5$. This is in contrast to the polycrystalline phase diagram (in green), in which the ferromagnetic phase persists up to $x = 0.5$. Data from refs 13 and 2. **b**,**c**, The resistivity is activated over all temperatures, being fitted to two exponentials.

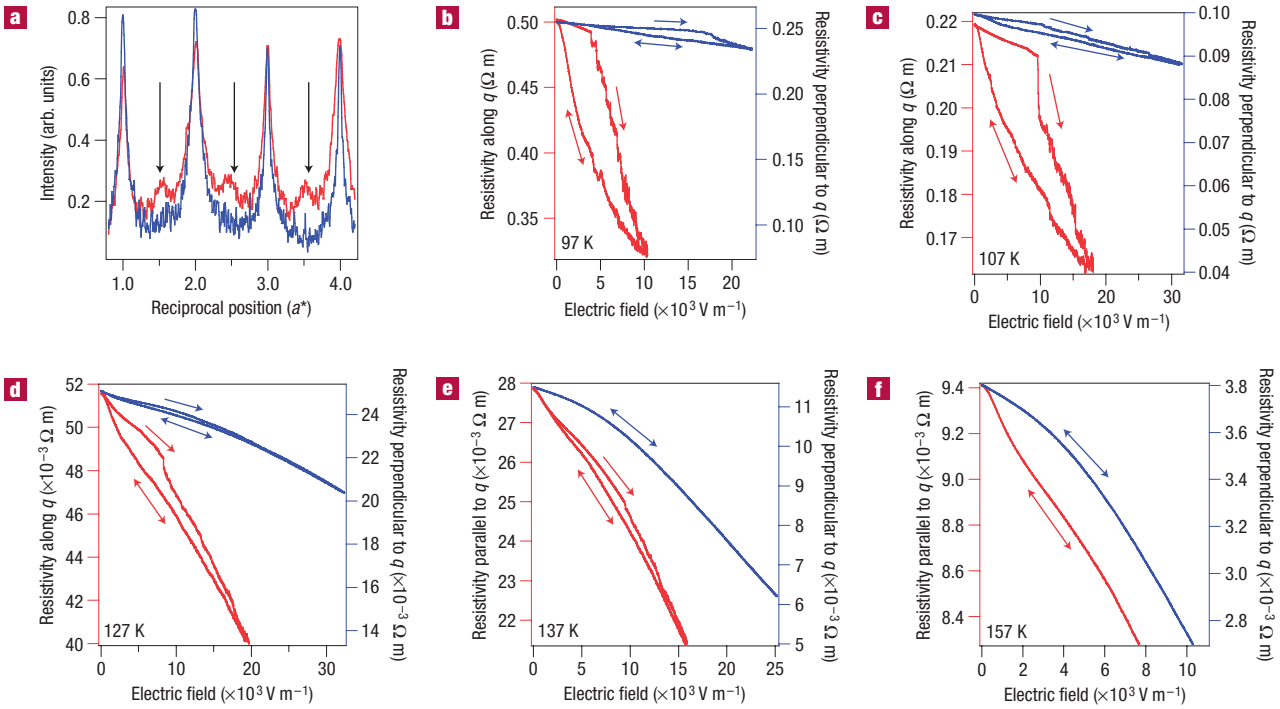

Figure 2 Variation of the differential resistance with current at different temperatures and with the current passed parallel and perpendicular to the superstructure. a, Linescan of TEM image in the **a** (red line) and **c** (blue line) directions showing the superstructure reflections present in only the **a** direction. **b–f**, Differential resistivity of $La_{0.5}Ca_{0.5}MnO_3$ versus d.c. bias with bias applied in the **a** (red lines) and **c** (blue lines) directions at various temperatures. In each case, the upper curve is the differential resistivity obtained after cycling the temperature to 300 K, and the lower curve is the path followed by subsequent bias sweeps.

ion beam microscope to a thickness of around 200 nm. The sample was examined in a Philips CM30 microscope and was cooled to 90 K using a Gatan liquid nitrogen stage. The uniaxial stripe phase was identified via superlattice reflections in a selected-area TEM diffraction pattern (illustrated in Fig. 2a); these reflections are detectable at 190 K, reaching a stable form at 90 K. (Note that previous resistivity measurements of thin-film $La_{0.5}Ca_{0.5}MnO_3$ have failed to produce consistent results[14–16], because of the difficulty of producing high-quality films and a failure to check for the superstructure using a microscopic technique.)

For the resistance measurements, gold wires were attached to the thin-film sample using graphite paint. The differential resistivity of the sample studied here was measured by using a lock-in amplifier to detect the a.c. voltage produced in response to a 17 Hz a.c. current plus a d.c. bias; contacts were placed around the edges of the film to enable the current and bias to be applied along different directions, chiefly parallel and perpendicular to the superlattice direction. Both four-point and two-point configurations were used for the resistivity experiments to eliminate possible contact resistance effects; the noise measurements reported below used two contacts.

Analogies between $La_{0.5}Ca_{0.5}MnO_3$ and other CDW systems are clearly apparent in Fig. 1, which shows the differential resistivity under zero d.c. bias versus temperature. The measurements appear similar to the resistivities of prototypical CDW systems doped with impurities[17,18], in that there is no clear feature at the expected CDW ordering temperature, with insulating behaviour (that is, decreasing resistivity with increasing temperature) persisting well above it. This has been interpreted as the 'smearing' of the transition caused by the large impurity density[17,18]. Analogous behaviour is also seen in cuprate ladder compounds exhibiting sliding density waves[19,20] below $T \simeq 200$ K. As in the case of the cuprates, the resistivity of $La_{0.5}Ca_{0.5}MnO_3$ shows an activated temperature dependence with an activation energy that varies from $\simeq$1,000–1,400 K (Fig. 1b,c).

Figure 2 shows the differential resistivity as a function of d.c. bias applied parallel (along the lattice vector **a**) and perpendicular (along the lattice vector **c**) to the superlattice direction. At 157 K (Fig. 2f), the differential resistivity drops in a similar fashion when the d.c. bias is applied in either direction. However, at temperatures $\lesssim$140 K, the differential resistivity undergoes a sharp drop when the bias is applied in the **a** direction; the effect is much less marked with the bias in the **c** direction (Fig. 2b–e). In addition, there is a large hysteresis between the differential resistance recorded when the bias is first applied in the **a** direction after cooling from 300 K, and that measured on subsequent bias sweeps (in Fig. 2b–e, the upper line in each direction shows the data from the first sweep after cooling and the lower line shows the data from subsequent sweeps); the area enclosed by the hysteresis loop increases rapidly as the temperature falls.

The hysteretic resistivity features shown in Fig. 2 are typical of CDWs in pinned and sliding states[10]. As the sample is cooled, the CDW settles into a minimum-free-energy pinned configuration, corresponding to maximum electrical resistivity[10]. On the application of electric field, the CDW initially undergoes local distortions that occur over longer and longer length scales as the field increases; eventually, the threshold field is reached and the CDW starts to slide. As the field is reduced again, the CDW freezes into a distorted state, characterized by a lower resistivity; the initial, minimum energy state cannot be regained without thermally cycling the sample[10], explaining the hysteresis in our data.

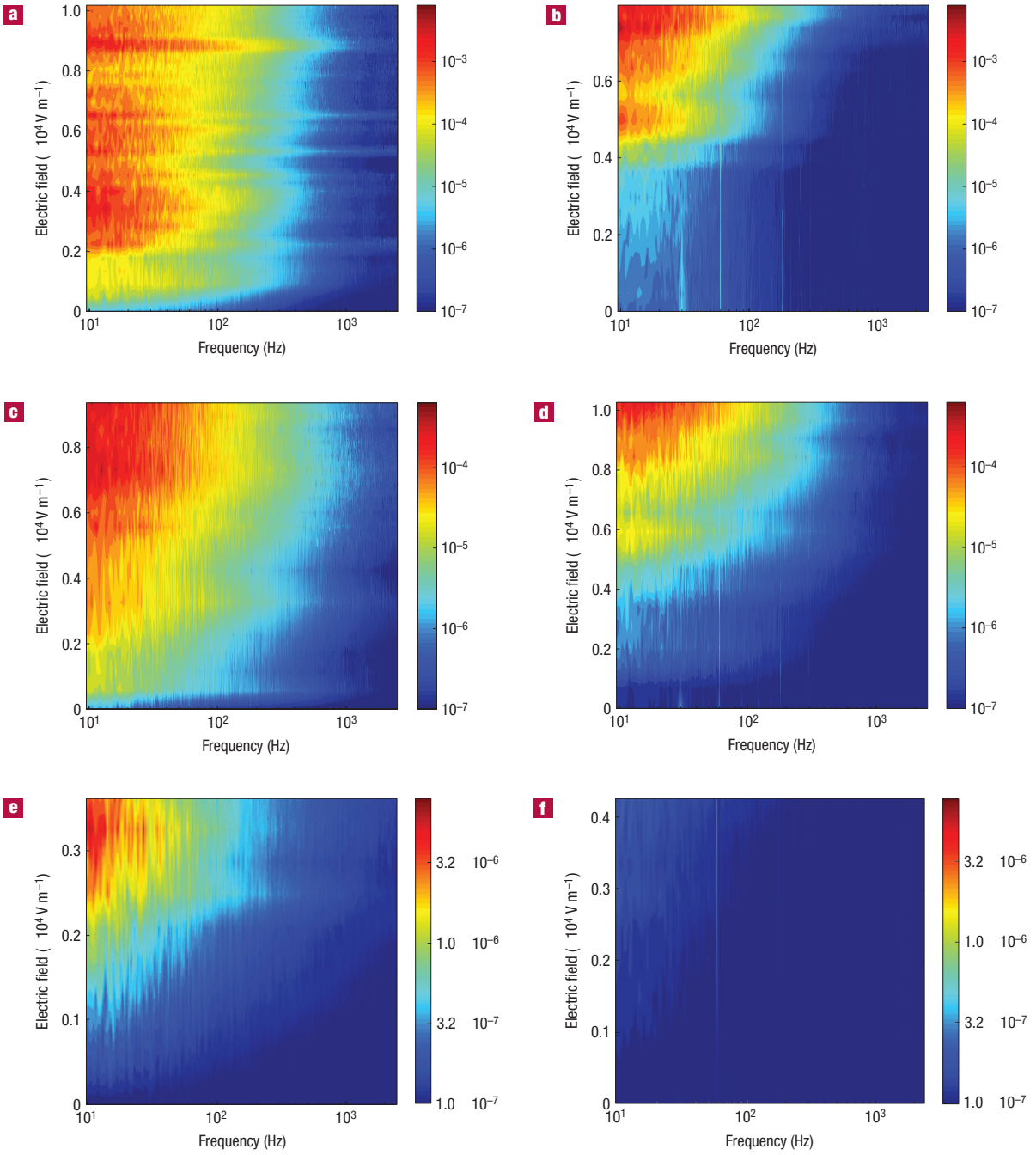

Figure 3 Frequency and current dependence of the broadband noise. a,**b**, 97 K data with the current parallel (**a**) and perpendicular (**b**) to *q*. **c**,**d**, 123 K data with the current parallel (**c**) and perpendicular (**d**) to *q*. **e**,**f**, 156 K data with the current parallel (**e**) and perpendicular (**f**) to *q*. The colour scale shows the magnitude of the power spectral density of the noise, in units of $V^2\,Hz^{-1}$.

Other mechanisms such as avalanche breakdown or sample heating cannot account for the data in Fig. 2. Although these effects might produce a falling differential resistivity as the field increases, they would not produce a history-dependent result; on removing the field, the sample would return to its initial state. Moreover, whereas the d.c. resistivity for currents in the **c** direction is two times higher than that for currents parallel to **a**, the drop in resistivity as the field increases is five times larger in the latter direction (Fig. 2); this anisotropy both fits naturally into the CDW picture and excludes heating and breakdown as possible mechanisms. The final model to consider is that of percolating ferromagnetic domains, which has been used successfully to describe the resistivity behaviour in the ferromagnetic manganites, particularly at the metal–insulator transition[21]. In the simple case of non-orientated domains, the anisotropy in the effects observed here rules out this mechanism. A more complex model with orientated domains is also ruled out as there is no evidence from the TEM data that a ferromagnetic phase is present (and indeed, it would be unexpected from the phase diagram, see Fig. 1a, inset). Finally, the model of percolating ferromagnetic domains can be ruled out

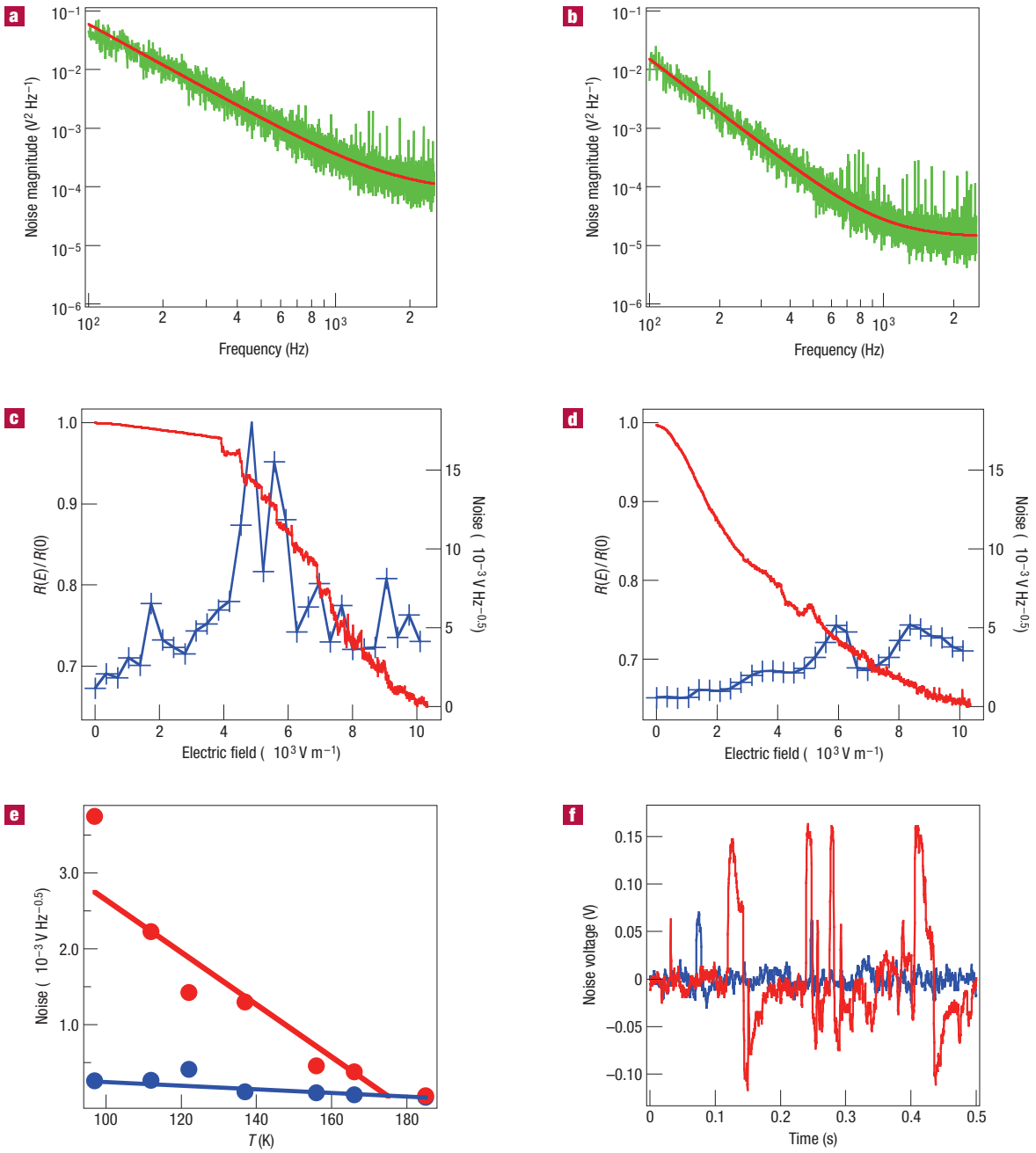

Figure 4 Variation of the magnitude of the noise with frequency, temperature and field, with the current passed parallel and perpendicular to the superstructure. **a**,**b**, Power spectral density of the noise with the current parallel (**a**) and perpendicular (**b**) to q. The data is shown in green, and a fit to a model of Johnson noise (a constant) plus broadband noise ($f^{-\alpha}$) is shown in red. **c**, Resistivity shown as $R(E)/R(0)$ (red line), and noise signal at 300 Hz (blue line) for the first time current is passed parallel to the superstructure after cooling from 300 K. **d**, Resistivity (red line) and noise (blue line) for the second time current is passed. **e**, Noise signal at 300 Hz and 10 V as a function of temperature in the superstructure (red line) and non-superstructure (blue line) directions. The noise at 300 Hz was extracted by calculating the power spectral density of the noise and then taking the square root. Twenty points of the power spectral density were averaged. **f**, Noise signal a short amount of time after the current has been changed; first (red line) and second (blue line) time the current is swept.

because the nonlinear resistivity shows activated behaviour for both low and high electric field biases, indicating that in both states the system is insulating, rather than one of the states having a strong metallic component.

Having explained the hysteresis when the bias is along **a**, we attribute the small amount of hysteresis seen when the bias is along **c** (Fig. 2) to imperfect contact geometry; that is, misalignment results in a small amount of bias being applied in the perpendicular direction.

It is initially surprising that it is possible to depin the CDW using moderate electric fields, as the expected wavevector of $q/a^* = 0.5$ (that is, commensurate with the lattice)[7,22] would

generally lead one to expect the CDW to be strongly locked to the lattice[23]. However, in the manganites it is well documented that the wavevector varies with increasing temperature[3] and from grain to grain within a polycrystalline sample[24]. These observations suggest that the energy gain from locking into the lattice must be relatively small, in accordance with the relatively low depinning fields observed.

Another distinguishing feature of CDWs is that they exhibit a broadband noise spectrum with an amplitude proportional to $f^{-\alpha}$, where f is the frequency[25–27]. Noise measurements were carried out in the range 10 Hz to 2.5 kHz using a low-noise current source. The noise signal was amplified with a high-input-impedance, low-noise preamplifier and was recorded via a digitizing oscilloscope. Lead capacitance, and the typical $10^6\ \Omega$ sample resistance, limited noise measurements to below 10 kHz. Other techniques commonly used on CDW systems such as $NbSe_3$ were considered or attempted but typical properties of manganite films rendered them impossible; manganite film resistivities and geometries lead to RC time constants that are too high to carry out experiments that measure effective pulse line or duration memory effects.

Figure 3 shows that significant broadband noise is observed in $La_{0.5}Ca_{0.5}MnO_3$ when the d.c. bias is applied in the superstructure direction. In contrast, the noise amplitude is much smaller when the bias is in the non-superstructure direction. The exponent α in $La_{0.5}Ca_{0.5}MnO_3$ runs from 0.8 (156 K) to 2.0 (100 K), a similar range to values seen in the prototypical CDW system $NbSe_3$ (0.8–1.8) (ref. 10). However, the magnitude of the broadband noise in $La_{0.5}Ca_{0.5}MnO_3$ is much larger than that observed in clean CDW systems; for $La_{0.5}Ca_{0.5}MnO_3$ the effective noise temperature at 300 Hz is $\sim 10^{11}$ K for a sample temperature of 100 K, whereas in pure $NbSe_3$ the effective noise temperature is $\sim 10^6$ K. This is attributable to the large amount of disorder present in $La_{0.5}Ca_{0.5}MnO_3$ (ref. 9; see above), so that there are many more pinning–depinning events compared with, for example, pure $NbSe_3$. Although broadband noise has previously been observed in impurity-pinned CDWs[28], narrowband noise has not been observed in an impurity-doped or radiation-damaged sample, probably because the width of the narrowband noise peak is proportional to the magnitude of the broadband noise[26]. Therefore, a high level of disorder or impurity pinning will lead to a large amount of broadband noise and unobservably small narrowband noise, as seen here in $La_{0.5}Ca_{0.5}MnO_3$.

In the well-tested Lee–Rice[29] model for a pinned CDW, the threshold field E_T can be used to estimate the characteristic pinning length L over which impurities or disorder deform the CDW sufficiently to pin it, that deformation being resisted by the elastic modulus κ of the CDW. We obtain $L = \sqrt{E_F/eE_TQ}$, and estimating a Fermi energy $E_F \sim 1$ eV (ref. 30), the threshold depinning field $E_T \sim 10^3\ \mathrm{V\,m^{-1}}$ (this work) and superstructure wavevector $Q \sim 10^{10}\ \mathrm{m^{-1}}$ (ref. 10), we find that $L \approx 300$ nm, much larger than the estimated impurity spacing[9], and justifying the weak pinning approximation. As a corollary, oscillation of the CDW in the pinned potential would be predicted to occur at a characteristic pinning frequency $\omega_p \sim (m/m_L)^{1/2}10^{12}$, which we estimate to be around 1 THz. This is in the same frequency range as an earlier reported feature in a striped manganite of a different composition, which was tentatively assigned to a pinned CDW mode[31].

As seen in other sliding CDW systems[27], the amount of broadband noise decreases with increasing temperature (Fig. 3a,c,e). For a bias above E_T ($\simeq 10^4\ \mathrm{V\,m^{-1}}$) in the superstructure direction, this decrease is approximately linear with temperature (Fig. 4c), as observed in the CDW system TaS_3 (ref. 27). With the bias in the non-superstructure direction, the noise increases much more slowly; at 100 K, it is more than an order of magnitude smaller than that with the bias along **a** (Fig. 4c). The small noise observed at high electric fields when the bias is along **c** is due to imperfect contact geometry, as discussed with regard to the differential resistance measurements above.

Figure 4a,b shows the variation of the broadband noise amplitude with applied bias between the first bias sweep after cooling from 300 K and on a subsequent sweep. On first biasing, the noise amplitude shows a large peak at the same point as the large fall in differential resistance (Fig. 4a). On subsequent bias sweeps, the noise increases more slowly with bias (Fig. 4b). The large peak during the first bias sweep is caused by a high level of random telegraph signal noise, which occurs in CDW systems as they switch from pinned to depinned states and back again[32,33] close to the threshold field. The distinctive shape of the random telegraph signal noise is shown in Fig. 4d, another factor adding weight to our identification of a CDW in $La_{0.5}Ca_{0.5}MnO_3$.

In summary, our resistivity and noise measurements strongly suggest that the superstructure in the stripe phase of manganites is a CDW that slides in the presence of an electric field. Such a manganite CDW would be a fully gapped system with no screening electrons, previously only observed in extremely clean organic materials[34]. However, our data suggest that the manganite CDW exists with a high level of impurities, leading to dramatic hysteresis effects in the resistance. Our findings call for a reanalysis of the large region of the manganite phase diagram, $0.5 \leq x < 0.85$, that is occupied by the stripe phase. In a wider context, this result is important because of the prevalence of stripe and chequerboard phases in oxide materials, including chelates, cobaltites, nickelates and cuprates; in particular, evidence is mounting that a glass of the stripe phase in cuprates may be linked to high-temperature superconductivity[1], making an understanding of the stripe phase a matter of urgency.

Received 30 June 2007; accepted 26 October 2007; published 2 December 2007.

References

1. Kohsaka, Y. *et al.* An intrinsic bond-centered electronic glass with unidirectional domains in underdoped cuprates. *Science* **315**, 1380–1385 (2007).
2. Cheong, S.-W. & Hwang, H. Y. in *Colossal Magnetoresistance Oxides* (ed. Tokura, Y.) Ch. 7, 237–280 (Gordon and Breach, London, 2000).
3. Chen, C. H., Mori, S. & Cheong, S.-W. Anomalous melting transition of the charge-ordered state in manganites. *Phys. Rev. Lett.* **83**, 4792–4795 (1999).
4. Chen, C. H. & Cheong, S.-W. Commensurate to incommensurate charge ordering and its real-space images in $La_{0.5}Ca_{0.5}MnO_3$. *Phys. Rev. Lett.* **76**, 4042–4045 (1996).
5. Chen, C. H., Cheong, S.-W. & Hwang, H. Y. Charge-ordered stripes in $La_{1-x}Ca_xMnO_3$ with $x > 0.5$. *J. Appl. Phys.* **81**, 4326–4330 (1997).
6. Mori, S., Chen, C. H. & Cheong, S.-W. Pairing of the charge-ordered stripes in $(La,Ca)MnO_3$. *Nature* **392**, 473–476 (1998).
7. Milward, G. C., Calderón, M. J. & Littlewood, P. B. Electronically soft phases in manganites. *Nature* **433**, 607–610 (2005).
8. Loudon, J. C. *et al.* Weak charge-lattice coupling requires reinterpretation of stripes of charge order in $La_{1-x}Ca_xMnO_3$. *Phys. Rev. Lett.* **94**, 097202 (2005).
9. Cox, S. *et al.* Evidence for the charge-density-wave nature of the stripe phase in manganites. *J. Phys. Condens. Matter* **19**, 192201 (2007).
10. Grüner, G. *Density Waves in Solids* (Addison-Wesley, Reading, 1994).
11. Majewski, P., Epple, L., Rozumek, M. & Schluckwerder, H. Phase diagram studies in the quasi binary systems $LaMnO_3$–$SrMnO_3$ and $LaMnO_3$–$CaMnO_3$. *J. Mater. Res.* **15**, 1161–1166 (2000).
12. Cox, S. *et al.* Strain control of superlattice implies weak charge-lattice coupling in $La_{0.5}Ca_{0.5}MnO_3$. *Phys. Rev. B* **73**, 132401 (2006).
13. Sanchez, D. *et al.* High resolution determination of ferromagnetic metallic limit in epitaxial $La_{1-x}Ca_xMnO_3$ films on $NdGaO_3$. *Appl. Phys. Lett.* **89**, 142509 (2006).
14. Butorin, S. M., Såthe, C., Saalem, F., Nordgren, J. & Zhu, X. M. Probing the Mn^{3+} sublattice in $La_{0.5}Ca_{0.5}MnO_3$ by resonant inelastic soft X-ray scattering at the Mn $L_{2,3}$ edge. *Surf. Rev. Lett.* **9**, 989–982 (2002).
15. Nyeanchi, E. B., Krylov, I. P., Zhu, X.-M. & Jacobs, N. Ferromagnetic ground state in $La_{0.5}Ca_{0.5}MnO_3$ thin films. *Eur. Phys. Lett.* **48**, 228–232 (1999).
16. Xiong, Y. M. *et al.* Magnetotransport properties in $La_{1-x}Ca_xMnO_3$ ($x = 0.33, 0.5$) thin films deposited on different substrates. *J. Appl. Phys.* **97**, 083909 (2005).
17. Ong, N. P. *et al.* Effect of impurities on the anomalous transport properties of $NbSe_3$. *Phys. Rev. Lett.* **42**, 811–814 (1979).
18. Chaikin, P. M. *et al.* Thermopower of doped and damaged $NbSe_3$. *Solid State Commun.* **39**, 553–557 (1981).
19. Blumberg, G. *et al.* Sliding density wave in $Sr_{14}Cu_{24}O_{41}$ ladder compounds. *Science* **297**, 584–587 (2002).
20. Maeda, A. *et al.* Sliding conduction by the quasi-one-dimensional charge-ordered state in $Sr_{14-x}Ca_xCu_{24}O_{41}$. *Phys. Rev. B* **67**, 115115 (2003).
21. Alers, G. B., Ramirez, A. P. & Jin, S. 1/f resistance noise in the large magnetoresistance manganites. *Appl. Phys. Lett.* **68**, 3644–3646 (1996).
22. Cox, S. *et al.* Very weak electron–phonon coupling and strong strain coupling in manganites. Preprint at <http://arxiv.org/abs/0704.2598> (2007).

23. Davis, T. A. *et al.* Evidence for a stress-induced incommensurate to commensurate charge-density-wave transition in TaS_3. *Phys. Rev. B* **39**, 10094–10100 (1989).
24. Loudon, J. C. *et al.* On the microstructure of the charge density wave observed in $La_{1-x}Ca_xMnO_3$. *Phil. Mag.* **85**, 999–1015 (2005).
25. Maeda, A., Naito, M. & Tanaka, S. Broad and narrow band noise of monoclinic TaS_3. *Solid State Commun.* **47**, 1001–1005 (1983).
26. Maher, M. P. *et al.* Size effects, phase slip, and the origin of $f^{-\alpha}$ noise in $NbSe_3$. *Phys. Rev. B* **43**, R9968–R9971 (1991).
27. Zettl, A. & Grüner, G. Broad band noise associated with the current carrying charge density wave state in TaS_3. *Solid State Commun.* **46**, 29–32 (1983).
28. Maeda, A., Uchinokura, K. & Tanaka, S. The effect of strong impurities on the low-frequency broad-band noise in $NbSe_3$. *Synth. Met.* **19**, 825–830 (1987).
29. Lee, P. A. & Rice, T. M. Electric field depinning of charge density waves. *Phys. Rev. B* **19**, 3970–3980 (1979).
30. Saitoh, T. *et al.* Temperature dependent pseudogaps in colossal magnetoresistive oxides. *Phys. Rev. B* **62**, 1039–1043 (2000).
31. Kida, N. & Tonouchi, M. Spectroscopic evidence for a charge-density-wave condensate in a charge-ordered manganite: Observation of a collective excitation mode in $Pr_{0.7}Ca_{0.3}MnO_3$ by using THz time-domain spectroscopy. *Phys. Rev. B* **66**, 024401 (2002).
32. Marley, A. C., Bloom, I. & Weissman, M. B. Temperature and electric-field dependences of characteristic noise patterns in mesoscopic ortho-TaS_3 charge density waves. *Phys. Rev. B* **49**, 16156–16161 (1994).
33. Bloom, I., Marley, A. C. & Weissman, M. B. Discrete fluctuators and broad-band noise in the charge-density-wave in $NbSe_3$. *Phys. Rev. B* **50**, 5081–5088 (1994).
34. McDonald, R. D. *et al.* Charge-density waves survive the Pauli paramagnetic limit. *Phys. Rev. Lett.* **93**, 076405 (2004).

Acknowledgements

We thank N. Harrison, N. D. Mathur, P. A. Midgley, G. Kotliar and E. Rosten for helpful comments. S.C. acknowledges support from the Seaborg Institute. The sample was grown and TEM was carried out at the University of Cambridge, where research was financially supported by the UK EPSRC. This research was financially supported by the US Department of Energy (DoE) under Grant LDRD-DR 20070013. Work at NHMFL is carried out under the auspices of the NSF, the State of Florida and the US DoE.
Correspondence and requests for materials should be addressed to S.C.